

Discovery of a Potent and Selective DGAT1 Inhibitor with a Piperidinyl-oxy-cyclohexanecarboxylic Acid Moiety

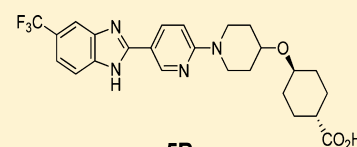
Shuwen He,* Qingmei Hong, Zhong Lai, David X. Yang, Pauline C. Ting, Jeffrey T. Kuethe, Timothy A. Cernak, Kevin D. Dykstra, Donald M. Sperbeck, Zhicai Wu, Yang Yu, Ginger X. Yang, Tianying Jian, Jian Liu, Deodial Guiadeen, Arto D. Krikorian, Lisa M. Sonatore, Judyann Wiltsie, Jinqi Liu, Judith N. Gorski, Christine C. Chung, Jack T. Gibson, JeanMarie Lisnock, Jianying Xiao, Michael Wolff, Sharon X. Tong, Maria Madeira, Bindhu V. Karanam, Dong-Ming Shen, James M. Balkovec, Shirly Pinto, Ravi P. Nargund, and Robert J. DeVita

Early Development and Discovery Sciences, Merck Research Laboratories, 2000 Galloping Hill Road, Kenilworth, New Jersey 07033, United States

Supporting Information

ABSTRACT: We report the discovery of a novel series of DGAT1 inhibitors in the benzimidazole class with a piperidinyl-oxy-cyclohexanecarboxylic acid moiety. This novel series possesses significantly improved selectivity against the A_{2A} receptor, no ACAT1 off-target activity at 10 μM , and higher aqueous solubility and free fraction in plasma as compared to the previously reported pyridyl-oxy-cyclohexanecarboxylic acid series. In particular, **5B** was shown to possess an excellent selectivity profile by screening it against a panel of more than 100 biological targets. Compound **5B** significantly reduces lipid excursion in LTT in mouse and rat, demonstrates DGAT1 mediated reduction of food intake and body weight in mice, is negative in a 3-strain Ames test, and appears to distribute preferentially in the liver and the intestine in mice. We believe this lead series possesses significant potential to identify optimized compounds for clinical development.

KEYWORDS: DGAT1, inhibitor, benzimidazole, ACAT1, A_{2A} receptor, cyclohexanecarboxylic acid, lipid tolerance test, epimerization, metabolite, Ames test, skin

**5B**

hDGAT ₁	IC ₅₀	3.9 nM
mDGAT ₁	IC ₅₀	23 nM
ACAT ₁	IC ₅₀	> 10 μM
A_{2A}	Ki	4.6 μM

DGAT1 inhibitors have emerged as potential therapeutic agents against diabetes and obesity.¹ DGAT (acyl CoA:diacylglycerol acyltransferase) catalyzes the final and committed step in the synthesis of triglyceride: the formation of triacylglycerol from diacylglycerol and acyl-CoA. DGAT1 is one of the isoforms and shares only limited homology with DGAT2 in the terms of amino acid sequence.^{2–4} DGAT1 has more sequence homology to acyl CoA:cholesterol acyltransferase (ACAT1 and ACAT2), which play a crucial role in cholesterol homeostasis.⁵ DGAT1 has attracted much attention since the disclosure of the phenotype of DGAT1 knockout mice, which were shown to be viable and resistant to diet-induced obesity.⁶ DGAT1 knockout mice were also reported to have enhanced insulin sensitivity compared to wild-type mice.⁷ The data, taken together, has prompted significant research effort in identifying small molecule DGAT1 inhibitors as a potential treatment for obesity and diabetes (Figure 1)^{8–16} In a phase II clinical trial, 3-week dosing of LCQ-908 (pradigastat) at 20 mg daily resulted in a 40% reduction in fasting triglyceride levels in patients with familial chylomicronemia syndrome, thus demonstrating the clinical proof of concept that inhibition of DGAT1 in humans leads to reductions of plasma triglycerides.¹⁷ Recent reports on the clinical results for AZD-7687 demonstrated the ability of DGAT1 inhibitors to attenuate postprandial triacylglyceride excursion. However, the gastrointestinal side effects could hinder further development of

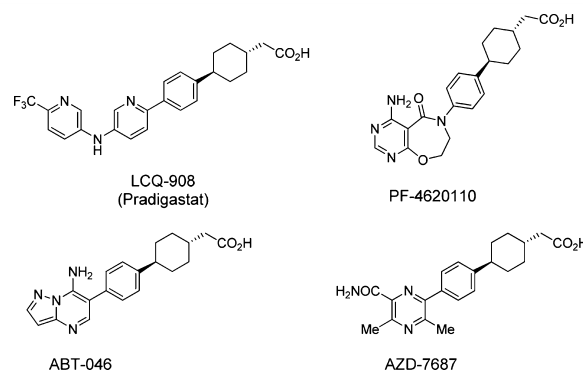


Figure 1. Structures of selected DGAT1 inhibitors.

DGAT1 inhibitors as a novel treatment for diabetes and obesity.^{18,19}

Recently, we disclosed a series of novel DGAT1 inhibitors in the benzimidazole class bearing a pyridyl-oxy-cyclohexanecarboxylic acid moiety.²⁰ A representative of this series, **1A**, is a potent DGAT1 inhibitor with excellent selectivity against

Received: February 9, 2014

Accepted: September 8, 2014

Published: September 8, 2014

ACAT1 (Figure 2). Furthermore, **1A** significantly reduces triglyceride excursion in lipid tolerance (LTT) in both mice

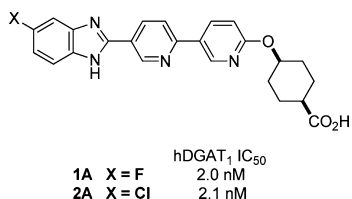


Figure 2. Representative DGAT1 inhibitors of the pyridyl-oxy-cyclohexanecarboxylic acid series.

and dogs. However, **1A** undergoes cis/trans isomerization in vivo, which could complicate the further development.

During the profiling of **1A** as the lead compound, other potential issues for this structural series were uncovered. First, **1A** has low aqueous solubility. In the high throughput solubility test, all the salt forms prepared, free form, formate, and ammonium salt, have solubility less than 10 μM in PBS buffers at pH 2 and 7, respectively. Second, **1A** appears to be tightly bound to plasma proteins. The unbound free fraction of **1A** in human plasma is only 0.36%. In mouse plasma, the unbound free fraction is slightly higher (1.7%). Finally, this series of compounds were shown to have an off-target interaction with the A_{2A} receptor.²¹ Compound **2A**, an earlier lead compound with a chloro substitution on the benzimidazole ring, was screened against a panel of known biological targets (Figure 2). In this test, **2A** had an IC₅₀ of 247 nM in a radioligand based competition binding assay with recombinant human A_{2A} receptor. The activity was later confirmed in a similar in-house human A_{2A} receptor binding assay. In this assay, **1A** had IC₅₀ of 334 nM, which is only ~160-fold selectivity against DGAT1. Consistent with this result, in an A_{2A} cAMP functional assay, compound **1A** displayed antagonist activity (IC₅₀ = 269 nM with 101% inhibition at 30 μM). Given the cis/trans isomerization issue and the potential issues discussed above, further profiling of **1A** was discontinued.

While profiling **1A** and related compounds, we continued to explore other structural variations to present both the benzimidazole and the carboxylic acid pharmacophores in the molecule. We became interested in a new design, which incorporates a piperidinyl linker instead of a pyridyl linker (e.g., structure **3A** in Figure 3). We believed the piperidinyl linker

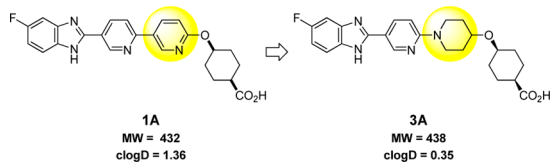


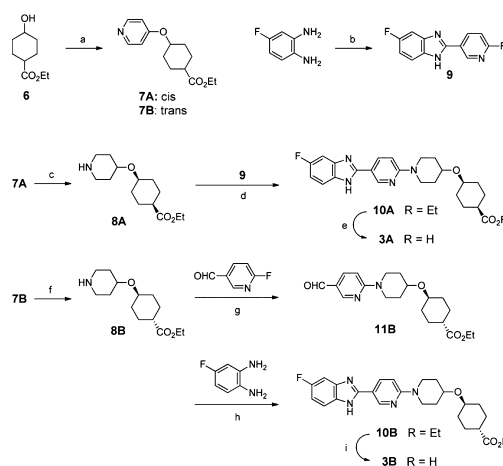
Figure 3. Design of the piperidinyl-oxy-cyclohexanecarboxylic acid series.

would impart more flexibility to the structure, as well as a more basic piperidine nitrogen, which could improve aqueous solubility with molecules of essentially the same molecular weight. As an advantage to alternative designs, the symmetrical nature of this piperidinyl linker would not impose additional stereochemical complications to the synthesis. Furthermore, given that many known A_{2A} receptor modulators have multiple aromatic rings in their structures, we expected that the saturation of the pyridyl ring system could decrease the number of aromatic rings and potentially reduce the affinity with the A_{2A} receptor.²²

In addition, the compounds with a piperidinyl linker series (e.g., **3A**) might have a lower risk to cause adverse effects in the skin. DGAT1 is known to be expressed in the skin of mice and human.²³ DGAT1 KO mice were shown to display deficiency in skin and fur, including sebaceous gland atrophy and hair loss. These findings raised concerns that pharmacological inhibition of DGAT1 in skin could lead to undesirable adverse effects in humans. The calculated logD for **3A** is about one unit lower than that of **1A** (0.35 vs 1.36, Figure 3). Given that the skin tissue is largely lipophilic, we believed that an inhibitor with lower logD is expected to distribute less in the skin and therefore has a lower tendency to elicit undesirable effect.²⁴

The synthesis for this series of compounds focused on the preparation of the piperidine substructures **8A** and its trans isomer **8B** (Scheme 1). The initial synthetic route involved

Scheme 1. Synthesis of **3A** and **3B**^a



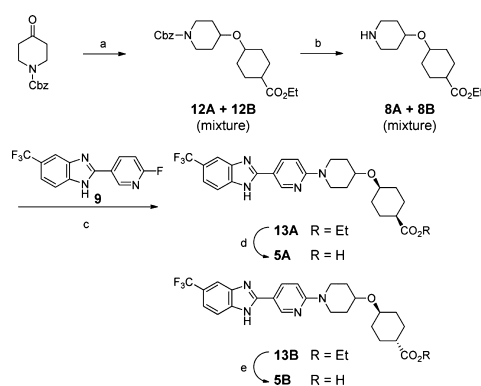
^aReagents and conditions: (a) 1. PPh₃, 4-hydroxypyridine, DIAD, THF, 55 °C, 2 days; 2. SFC (ChiralPak AD-H), **7A** (14% for two steps), **7B** (23% for two steps); (b) 6-fluoronicotinaldehyde, potassium peroxymonosulfate, DMF–water, 69%; (c) PtO₂, TsOH, H₂ (45 psi), EtOH, RT, 5 days; (d) NaHCO₃, DMSO, 110 °C, 43% for two steps; (e) LiOH, THF–water, 83%; (f) PtO₂, TsOH, H₂ (45 psi), EtOH, 5 days; (g) NaHCO₃, DMSO, 110 °C, 27% for two steps; (h) potassium peroxymonosulfate, 4-fluorobenzene-1,2-diamine, DMF–water, 18%; (i) LiOH, THF–water, 70%.

saturation a pyridyl ring to furnish the required piperidinyl intermediates. The Mitsunobu reaction of commercially available ethyl 4-hydroxycyclohexanecarboxylate **6** (a cis and trans mixture) and 4-hydroxypyridine followed by SFC separation gave the cis and trans isomers (**7A** and **7B**). Saturation of the pyridyl ring to a piperidinyl ring turned out to be challenging, which we rationalized to be due to the electron donating effect of the alkoxy substituent on 4-position of the pyridyl ring. Eventually, we were able to hydrogenate **7A** to piperidine **8A** with frustratingly long reaction time at 45 psi in a Parr shaker at room temperature. The trans isomer **7B** behaved similarly in the hydrogenation step to give **8B**. Coupling of **8A** with 2-(6-fluoropyridin-3-yl)-5-fluoro-1H-benzimidazole **9** gave ethyl ester **10A**. The coupling reaction condition was identified from a comprehensive screening of a variety of solvents and bases. Eventually, we identified that the coupling worked best with a weak inorganic base such as NaHCO₃ in polar aprotic solvents (such as DMSO and NMP).²⁵ The coupling chemistry thus developed proved to be pivotal for the rapid progression of this structural series. Under the same conditions, **8B** was coupled

with 6-fluoronicotinaldehyde to give aldehyde intermediate **11B**. Oxidative condensation of **11B** with 4-fluorobenzene-1,2-diamine afforded ester **10B**. Finally, hydrolysis of ethyl esters **10A** and **10B** provided compounds **3A** and **3B**, respectively.

The difficulty in preparing the piperidine pieces (**8A** and **8B**) by the route shown above significantly hampered the synthesis and profiling of this series of compounds. To overcome this synthetic problem, we developed a new route starting with benzyl 4-oxopiperidine-1-carboxylate (Scheme 2). Reductive

Scheme 2. Reductive Etherification Route^a



^aReagents and conditions: (a) 1. ethyl 4-hydroxycyclohexanecarboxylate (cis/trans mixture), triethylamine, TMSCl, 0 °C; 2. benzyl 4-oxopiperidine-1-carboxylate, Et₃SiH, TMSOTf, -78 to 0 °C, 91%; (b) 1. H₂, Pd/C; 2. NaHCO₃, NMP, 110 °C; 3. SFC (ChiralPak AD-H), **13A** (37% for three steps), **13B** (33% for three steps); (d) LiOH, THF–water, RT, 73%; (e) LiOH, THF–water, RT, 81%.

etherification of this starting material with ethyl 4-hydroxycyclohexanecarboxylate (cis and trans) gave a mixture of **12A** and **12B**.²⁶ Removal of Cbz-protecting group using standard conditions furnished a mixture of **8A** and **8B**. Following the chemistry described above, **5A** and **5B** were prepared. During the reductive etherification reaction, trans/cis configuration in ethyl 4-hydroxycyclohexanecarboxylate was transferred to the product with complete retention. Therefore, scale-up of this series of compounds could begin with pure *cis*- or *trans*-ethyl 4-hydroxycyclohexanecarboxylate to provide the desired intermediate in *cis* or *trans* form, respectively.²⁷

Applying the chemistry described above, we prepared the compounds with several different substitutions on the benzimidazole ring in both the *cis* and *trans* series. The compounds and their profiles are listed in Table 1. Most of the

compounds in piperidinyl series maintain potent inhibition on both human and mouse DGAT1 except for **3B**, the least potent analogue in this series.²⁸ The compounds are slightly less potent on mouse DGAT1 than on human DGAT1. The potency loss appears to be more severe for the compounds in the *trans* series. In contrast, in the pyridyl linked series reported earlier (e.g., **1A**), there is less differentiation of potencies (human vs mouse and *cis* vs *trans*).¹⁶ However, the piperidinyl series shows much improved off-target selectivity. All the compounds in the piperidinyl series are now highly selective against ACAT1.²⁹ In contrast, in the pyridyl linker series, a small substituent on benzimidazole (e.g., F or H) is required to offer good ACAT selectivity, while maintaining potent DGAT1 inhibition. Furthermore, all the piperidinyl linked compounds possess improved selectivity against A_{2A} as compared to **1A** and **2A** of the pyridyl linker series. In particular, **3A**, **4B**, **5A**, and **5B** achieve >1000-fold selectivity (the ratios of hDGAT1 IC₅₀ and hA_{2A} K_i). Finally, the piperidinyl series displays improved aqueous solubility and increased free fractions in plasma. For example, the TFA salt of **5B** has solubility of 130 and 151 μM in PBS buffer at pH 2 and 7, respectively. The solubility of the free form is 167 μM and 153 μM at pH 2 and 7, respectively. The free fraction of **5B** is 9.0% and 7.8% in human and mouse plasma, respectively.³⁰

The compounds were subsequently tested in rodent lipid tolerance test (LTT), an *in vivo* lipid excursion assay, to evaluate their ability to inhibit plasma triglyceride accumulation. In mouse LTT screening at 10 mpk oral dose, **3A** and **4A** show modest efficacy reducing lipid excursion (~50% at 20 h time point).³¹ Because of its poor potency on mouse DGAT1, **3B** was excluded from mouse LTT screening. However, **5A** and **5B** with a CF₃ substituent have the best efficacy. Similarly, **4B** with a chloro substituent on benzimidazole ring gave excellent efficacy in mouse LTT screening. However, it suffers from slightly increased off-target activity on hERG ion channel in a competitive binding assay with radiolabeled MK-499 (K_i = 4.0 μM).³² Because of its excellent efficacy observed in mouse LTT screening, **5B** was also tested in rat LTT model (Figure 4).³³ At 1 mpk and 3 mpk, **5B** reduces lipid excursion in rat by ~80%. The corresponding plasma concentrations of **5B** were 20 and 58 nM.³⁴ In this assay, reduction of lipid excursion by the positive control, Cpd A (a known DGAT1 inhibitor from the literature), at 10 mpk was normalized to 100%.³⁵

To establish the target engagement on DGAT1, **5B** was evaluated in wild type (WT) vs DGAT1 knockout (KO) mice for the effect on body weight and food intake (Figure 5).³⁶ In a six day study with daily dosing at 10 mpk, **5B** reduced cumulative

Table 1. Profiles of Compounds 3–5

compd	cis/ trans	X	human DGAT1 IC ₅₀ (nM)	mouse DGAT1 IC ₅₀ (nM)	human ACAT1 IC ₅₀ (% inh. at 10 μM)	hA _{2A} binding K _i (μM)	mouse LTT (10 mpk) triglyceride reduction @18 h	hERG binding (K _i , μM)
3A	cis	F	5.8	26	>10 μM (-2%)	>10	55%	11
3B	trans	F	15	110	>10 μM (5%)	9.7	ND	>60
4A	cis	Cl	2.2	11	>10 μM (13%)	ND	52%	15
4B	trans	Cl	2.9	29	>10 μM (4%)	3.5	75%	4.0
5A	cis	CF ₃	2.5	8.0	>10 μM (22%)	8.0	75%	7.0
5B	trans	CF ₃	3.9	23	>10 μM (23%)	4.6	89%	10

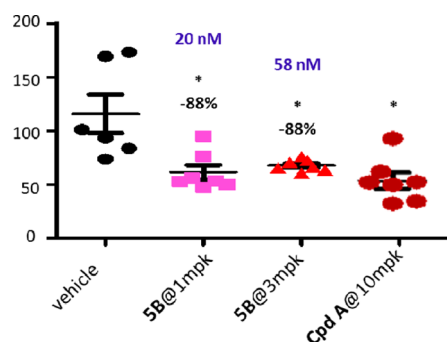


Figure 4. Compound **5B** reduces lipid excursion in rat LTT.

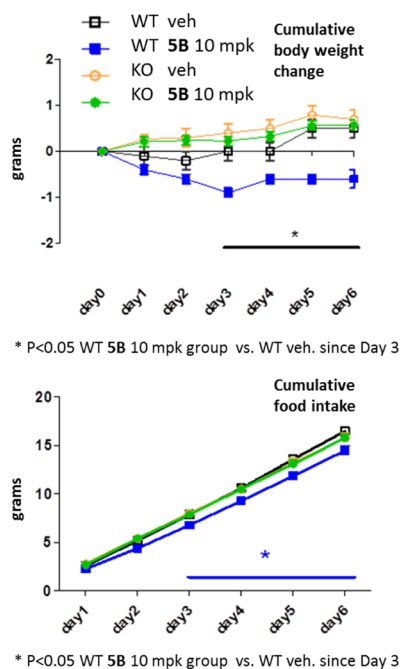


Figure 5. Effect on body weight and food intake of **5B** in DGAT1 KO vs WT mice.

body weight gain and food intake significantly in WT mice as compared to vehicle treated groups starting from day 3, while the body weight and food intake of **5B** treated KO mice were indistinguishable from the vehicle treated group. This result strongly suggests that the reduction of body weight and food intake was due to the inhibition of DGAT1.

During the profiling of **5B**, there was some concern around the possible mutagenicity due to the presence of a benzimidazole moiety in the structure.³⁷ Initial in silico prediction by MultiCASE and DEREK indicated that the probability of mutagenicity was low.³⁸ Indeed, **5B** was tested and shown to be negative in a 3-strain microbial mutagenesis assay. Over a concentration range of 30 to 5000 $\mu\text{g}/\text{plate}$, **5B** did not produce any 2-fold or greater increases in revertants relative to the solvent control in any of the three strains tested (TA1535, TA98, and TA100), either with or without metabolic activation. This result offered us more confidence on the overall potential for this structure class.

With the increasing interest in **5B** as a potential development candidate, **5B** was screened against a panel of more than 100 biological targets (receptors and enzymes). In this set of assays, **5B** showed an excellent selectivity profile with $\text{IC}_{50} > 10 \mu\text{M}$ against all targets except $\text{A}_{2\text{A}}$.

As **5B** was extensively profiled as a potential development candidate, **1A** in the pyridyl linked series was shown to isomerize to its trans isomer in vivo. Immediately, **5B** was evaluated for this possibility. In a hepatocyte incubation study, **5B** does isomerize but at different levels across the species (Table 2). In dog and

Table 2. Conversion of **5B** to **5A** and Vice Versa in Hepatocyte Incubation^a

conversion of 5B (parent) to 5A (metabolite)	
species	5A peak area as % of 5B
mouse	3.3%
rat	34.6%
dog	0%
monkey	0%
human	5.7%
conversion of 5A (parent) to 5B (metabolite)	
species	5B peak area as % of 5A
rat	67.0%
human	26.1%

^aCompound was added with final concentration of 10 μM into hepatocytes diluted to 1×10^6 cell/mL in a buffer. The incubation was performed at 37 °C for 120 min. The plates were centrifuged, and the supernatant was analyzed by LC–MS/MS.

monkey, the isomerization was minimal, while in mouse and human there was more isomerization. The isomerization was most pronounced in rat hepatocytes. As a comparison, the isomerization from **5A** (the cis isomer) to *trans*-**5B** occurs more extensively in rat and human.

In addition to the in vitro hepatocyte incubation study, **5B** was also tested for its in vivo pharmacokinetics in rat and dog (Table 3). Consistent with the in vitro data, about half of *trans*-**5B** was

Table 3. Pharmacokinetic Data for **5B** in Rat and Dog^{a,b}

PK parameters	rat	dog
<i>F</i> (%)	8	126
<i>Cl</i> ($\text{mL min}^{-1} \text{kg}^{-1}$)	5.82	88.9
<i>V</i> _{dss} (L kg^{-1})	0.19	4.54
<i>t</i> _{1/2} (h)	0.91	1.16
oral dose (mg kg^{-1})	2	4
AUC ($\mu\text{M}\cdot\text{h}$) 5B	1.00	1.94
AUC ($\mu\text{M}\cdot\text{h}$) metabolite 5A	0.97	0.11

^aCompound **5B** was dosed in Sprague–Dawley rats as a solution in EtOH/PEG400/water (10:50:40) at 1 mg/kg, iv, and 2 mg/kg, po.

^bCompound **5B** was dosed in beagle dogs as a solution in 30% captisol (pH 8) at 1 mg/kg, iv, and in 0.5 methylcellulose at 4 mg/kg, po.

converted to the cis isomer **5A** in rat in vivo as indicated by the AUCs in plasma. Less isomerization occurred in dog (~5%).

Finally, **5B** was dosed orally in mice to determine the distribution in various tissues of interest (Table 4). Considering the isomerization of **5B** to **5A**, the drug levels of **5A** were also measured. Compound **5B** showed much higher drug levels in liver and small intestine compared with the concentrations in plasma at both 3 and 24 h time points. The level of **5B** in skin is much lower compared to liver and intestine, but still high compared with the IC_{50} on DGAT1 (17- and 7-fold over mouse DGAT1 IC_{50} at 3 and 24 h, respectively). The tissue distribution of **5A** (the metabolite of **5B** from isomerization) tracks that of **5B** albeit at lower concentrations. On the basis of this study, **5B** demonstrated favorable distributions in the target organs (liver

Table 4. Mouse Tissue Distribution after Oral Dosing of 5B^a

tissue	concentration of 5B (μM)		concentration of 5A (μM)	
	3 h	24 h	3 h	24 h
plasma	0.324	<0.01	0.054	<0.01
liver	21.6	4.02	6.91	0.672
intestine (small)	36.6	0.711	5.026	0.076
fat (adipose)	0.237	<0.01	0.021	<0.010
skin	0.404	0.167	0.046	0.018

^aCompound 5B was dosed in C57BL/6 mice as a solution in EtOH/PEG400/water (10:50:40) at 10 mg/kg, po.

and small intestine). However, 5B is present in the skin at a significant concentration. Furthermore, the isomerization of 5B to an active metabolite (5A) could complicate the development process.³⁹ Therefore, although there were many desirable attributes associated with 5B, the profiling of 5B as a potential development candidate was discontinued.

In summary, we have described the discovery of a novel series of DGAT1 inhibitors in the benzimidazole class with a piperidinyl-oxy-cyclohexanecarboxylic acid moiety. This series of compounds abolish the ACAT1 off-target activity associated with the earlier pyridyl-oxy-cyclohexanecarboxylic acid series. Meanwhile, the liability of A_{2A} binding affinity is significantly reduced by the introduction of the piperidinyl linker. The series shows improved aqueous solubility and higher free fraction in plasma. The most interesting compound in this series to date, 5B, was shown to possess an excellent selectivity profile by screening it against a panel of more than 100 biological targets. In addition to its favorable in vitro profile, 5B significantly reduced lipid excursion in LTT assays in mouse and rat, respectively. In a WT vs DGAT1 KO mouse study, 5B demonstrated DGAT1 mediated reduction in food intake and body weight. Upon oral dosing in mice, 5B seemed to distribute in liver and small intestine preferentially. Furthermore, the risk of mutagenicity of 5B was low based on a 3-strain Ames test. All the exciting data collected for 5B helped us to make a critical decision to deprioritize the previous pyridyl linked series and instead focus on this new series. Additional efforts focusing on addressing cis/trans isomerization issue and further reducing the distribution of the DGAT1 inhibitor in skin while maintaining other desirable attributes will be disclosed in the future.

■ ASSOCIATED CONTENT

Ⓢ Supporting Information

Syntheses and characterization data for the new compounds. This material is available free of charge via the Internet at <http://pubs.acs.org>.

■ AUTHOR INFORMATION

Corresponding Author

*(S.H.) Phone: 908-740-0881. E-mail: shuwen_he@merck.com.

Notes

The authors declare no competing financial interest.

■ ACKNOWLEDGMENTS

We thank Mr. Thomas J. Novak and Dr. Li-Kang Zhang at Merck Research Laboratories for measuring the high resolution mass.

■ REFERENCES

- (1) Birch, A. M.; Buckett, L. K.; Turnbull, A. V. DGAT1 inhibitors as anti-obesity and anti-diabetic agents. *Curr. Opin. Drug Discovery Dev.* **2010**, *13*, 489–496.
- (2) Cases, S.; Smith, S. J.; Zheng, Y.-W.; Myers, H. M.; Lear, S. R.; Sande, E.; Novak, S.; Collins, C.; Welch, C. B.; Lusis, A. J.; Erickson, S. K.; Farese, R. V., Jr. Identification of a gene encoding an acyl CoA:diacylglycerol acyltransferase, a key enzyme in triacylglycerol synthesis. *Proc. Natl. Acad. Sci. U.S.A.* **1998**, *95*, 13018–13023.
- (3) Cases, S.; Stone, S. J.; Zhou, P.; Yen, E.; Tow, B.; Lardizabal, K. D.; Voelker, T.; Farese, R. V., Jr. Cloning of DGAT2, a second mammalian diacylglycerol acyltransferase, and related family members. *J. Biol. Chem.* **2001**, *276*, 38870–38876.
- (4) Yen, C. E.; Stone, S. J.; Koliwad, D.; Harris, C.; Farese, R. V., Jr. DGAT enzymes and triacylglycerol biosynthesis. *J. Lipid Res.* **2008**, *49*, 2283–2301.
- (5) Pramfalk, C.; Eriksson, M.; Parini, P. Cholesteryl esters and ACAT. *Eur. J. Lipid Sci. Technol.* **2012**, *114*, 624–633.
- (6) Smith, S. J.; Cases, S.; Jensen, D. R.; Chen, H. C.; Sande, E.; Tow, B.; Sanan, D. A.; Raber, J.; Eckel, R. H.; Farese, R. V., Jr. Obesity resistance and multiple mechanisms of triglyceride synthesis in mice lacking Dgat. *Nat. Genet.* **2000**, *25*, 87–90.
- (7) Chen, H. C.; Rao, M.; Sajan, M. P.; Standaert, M.; Kanoh, Y.; Miura, A.; Farese, R. V., Jr. Role of adipocyte-derived factors in enhancing insulin signaling in skeletal muscle and white adipose tissue of mice lacking Acyl CoA:diacylglycerol acyltransferase 1. *Diabetes* **2004**, *53*, 1445–1451.
- (8) For recent reports of DGAT1 inhibitors, see: Serrano-Wu, M. H.; Kwak, Y.; Coppola, G.; Foster, C.; Gilmore, T.; Gong, Y.; He, G.; Hou, Y.; Kantor, A.; Li, J.; Mergo, W.; Nakajima, K.; Neubert, A.; Radetich, B.; Stroup, B.; Sung, M.; Szklennik, P.; Tichkule, R.; Yang, L.; Yoon, T.; Zhu, Y.; Wareing, J.; Hosagrahara, V.; Jain, M.; Chatelain, R.; Commerford, R.; Dardik, B.; Meyers, D.; Hubbard, B. Discovery of a DGAT1 inhibitor with robust suppression of postprandial triglyceride levels in humans. Abstracts of Papers, 243rd ACS National Meeting & Exposition, San Diego, CA, March 25–29, 2012.
- (9) Serrano-Wu, M. H.; Coppola, G. M.; Gong, Y.; Neubert, A. D.; Chatelain, R.; Clairmont, K. B.; Commerford, R.; Cosker, T.; Daniels, T.; Hou, Y.; Jain, M.; Juedes, M.; Li, L.; Mullarkey, T.; Rocheford, E.; Sung, M. J.; Tyler, A.; Yang, Q.; Yoon, T.; Hubbard, B. K. Intestinally targeted diacylglycerol acyltransferase 1 (DGAT1) inhibitors robustly suppress postprandial triglycerides. *ACS Med. Chem. Lett.* **2012**, *3*, 411–415.
- (10) Dow, R. L.; Li, J.-C.; Pence, M. P.; Gibbs, E. M.; LaPerle, J. L.; Litchfield, J.; Piotrowski, D. W.; Munchhof, M. J.; Manion, T. B.; Zavadski, W. J.; Walker, G. S.; McPherson, R. K.; Tapley, S.; Sugarman, E.; Guzman-Perez, A.; Dasilva-Jardine, P. Discovery of PF-04620110, a potent, selective, and orally bioavailable inhibitor of DGAT-1. *ACS Med. Chem. Lett.* **2011**, *2*, 407–412.
- (11) Yeh, V. S.; Beno, D. W.; Brodjian, S.; Brune, M. E.; Cullen, S. C.; Dayton, B. D.; Dhaon, M. K.; Falls, H. D.; Gao, J.; Grihalde, N.; Hajduk, P.; Hansen, T. M.; Judd, A. S.; King, A. J.; Klux, R. C.; Larson, K. J.; Lau, Y. Y.; Marsh, K. C.; Mittelstadt, S. W.; Plata, D.; Rozema, M. J.; Segreti, J. A.; Stoner, E. J.; Voorbach, M. J.; Wang, X.; Xin, X.; Zhao, G.; Collins, C. A.; Cox, B. F.; Reilly, R. M.; Kym, P. R.; Souers, A. J. Identification and preliminary characterization of a potent, safe, and orally efficacious inhibitor of acyl-CoA:diacylglycerol acyltransferase 1. *J. Med. Chem.* **2012**, *55*, 1751–1757.
- (12) Plowright, A. T.; Barton, P.; Stuart, B.; Alan, M.; Birtles, S.; Buckett, L. K.; Butlin, R. J.; Davies, R. D. M.; Ertan, A.; Gutierrez, P. M.; Kemmitt, P. D.; Leach, A. G.; Svensson, P. H.; Turnbull, A. V.; Waring, M. J. Design and synthesis of a novel series of cyclohexyloxy-pyridyl derivatives as inhibitors of diacylglycerol acyl transferase 1. *Med. Chem. Commun.* **2013**, *4*, 151–158.
- (13) Barlund, J. G.; Bauer, U. A.; Birch, A. M.; Birtles, S.; Buckett, L. K.; Butlin, R. J.; Davies, R. D. M.; Eriksson, J. W.; Hammond, C. D.; Hovland, R.; Johannesson, P.; Johansson, M. J.; Kemmitt, P. D.; Lindmark, B. T.; Morentin, P.; Noesk, T. A.; Nordin, A.; O'Donnell, C. J.; Petersson, A. U.; Redzic, A.; Turnbull, A. V.; Vinblad, J. Design and

optimization of pyrazinecarboxamide-based inhibitors of diacylglycerol acyltransferase 1 (DGAT1) leading to a clinical candidate dimethylpyrazinecarboxamide phenylcyclohexylacetic acid (AZD7687). *J. Med. Chem.* **2012**, *55*, 10610–10629.

(14) Waring, M. J.; Birch, A. M.; Birtles, S.; Buckett, L. K.; Butlin, R. J.; Campbell, L.; Gutierrez, P. M.; Kemmitt, P. D.; Leach, A. G.; MacFaul, P. A.; O'Donnell, C.; Turnbull, A. V. Optimisation of biphenyl acetic acid inhibitors of diacylglycerol acetyl transferase 1: the discovery of AZD2353. *Med. Chem. Commun.* **2013**, *4*, 159–164.

(15) Goldberg, F. W.; Birch, A. M.; Leach, A. G.; Groombridge, S. D.; Snelson, W. L.; Gutierrez, P. M.; Hammond, C. D.; Birtles, S.; Buckett, L. K. Discovery and optimization of efficacious neutral 4-amino-6-biphenyl-7,8-dihydropyrimido[5,4-f][1,4]oxazepin-5-one diacylglycerol acyl transferase-1 (DGAT1) inhibitors. *Med. Chem. Commun.* **2013**, *4*, 165–174.

(16) DeVita, R. J.; Pinto, S. Current status of the research and development of diacylglycerol O-acyltransferase 1 (DGAT1) inhibitors. *J. Med. Chem.* **2013**, *56*, 9820–9825.

(17) Meyers, C.; Gaudet, D.; Tremblay, K.; Amer, A.; Chen, J.; Aimin, F. The DGAT1 inhibitor LCQ908 decreases triglyceride levels in patients with the familial chylomicronemia syndrome. *J. Clin. Lipidol.* **2012**, *6*, 266–267.

(18) Denison, H.; Nilsson, C.; Kujacic, M.; Löfgren, L.; Karlsson, C.; Knutsson, M.; Eriksson, J. W. Proof of mechanism for the DGAT1 inhibitor AZD7687: results from a first-time-in-human single-dose study. *Diabetes Obes. Metab.* **2013**, *15*, 136–143.

(19) Denison, H.; Nilsson, C.; Löfgren, L.; Himmelmann, A.; Mårtensson, G.; Knutsson, M.; Al-Shurbaji, A.; Tornqvist, H.; Eriksson, J. W. Diacylglycerol acyltransferase 1 inhibition with AZD7687 alters lipid handling and hormone secretion in the gut with intolerable side effects: a randomized clinical trial. *Diabetes Obes. Metab.* **2014**, *16*, 334–343.

(20) He, S.; Hong, Q.; Lai, Z.; Wu, Z.; Yu, Y.; Kim, D. W.; Ting, P. C.; Kuethe, J. T.; Yang, G. X.; Jian, T.; Liu, J.; Guideen, D.; Krikorian, A. D.; Sperbeck, D. M.; Sonatore, L. M.; Wiltse, J.; Chung, C. C.; Gibson, J. T.; Lisnock, J.; Murphy, B. A.; Gorski, J. N.; Liu, J.; Chen, D.; Chen, X.; Wolff, M.; Tong, S. X.; Madeira, M.; Karanam, B. V.; Shen, D.-M.; Balkovec, J. M.; Pinto, S.; Nargund, R. P.; DeVita, R. J. *ACS Med. Chem. Lett.* **2013**, *4*, 773–778.

(21) A_{2A} receptor mediates many important physiological functions. de Lera Ruiz, M.; Lim, Y.-H.; Zheng, J. Adenosine A_{2A} receptor as a drug discovery target. *J. Med. Chem.* **2014**, *57*, 3623–3650.

(22) For a review on small molecule adenosine receptor agonists and antagonists, see: Müller, C. E.; Jacobson, K. A. Recent developments in adenosine receptor ligands and their potential as novel drugs. *Biochim. Biophys. Acta* **2011**, *1808*, 1290–1308.

(23) Chen, H. C.; Smith, S. J.; Tow, B.; Elias, P. M.; Farese, R. V. Leptin modulates the effects of acyl CoA:diacylglycerol acyltransferase deficiency on murine fur and sebaceous glands. *J. Clin. Invest.* **2002**, *109*, 175–181.

(24) Subsequently, we carried out a study to evaluate logD as a predictor of skin exposure with subsequent induction of sebaceous gland atrophy: Muise, E. S.; Zhu, Y.; Verras, A.; Karanam, B. V.; Gorski, J.; Weingarh, D.; Lin, H. V.; Hwa, J.; Thompson, J. R.; Hu, G.; Liu, J.; He, S.; DeVita, R. J.; Shen, D.-M.; Pinto, S. Identification and characterization of sebaceous gland atrophy-sparing DGAT1 inhibitors. *PLoS One* **2014**, *9*, e88908.

(25) For a report detailing the effort identifying the optimal coupling condition, see: Cernak, T. A.; et al. Manuscript in preparation.

(26) For an initial disclosure of the reductive etherification as an efficient strategy to prepare ether compounds, see: Hatakeyama, S.; Mori, H.; Kitano, K.; Yamada, H.; Nishizawa, M. Efficient reductive etherification of carbonyl compounds with alkoxytrimethylsilanes. *Tetrahedron Lett.* **1994**, *35*, 4367–4370.

(27) For a report on the application of the reductive etherification strategy for the preparation of **12A**, **12B**, and related compounds, see: Kuethe, J. T.; Janey, J. M.; Truppo, M.; Arradondo, J.; Li, T.; Yong, K.; He, S. A biocatalytic/reductive etherification approach to substituted piperidyl ethers. *Tetrahedron* **2014**, *70*, 4563–4570.

(28) For a description of the protocols for enzyme inhibition assays, see: Liu, J.; Gorski, J. N.; Gold, S. J.; Chen, D.; Chen, S.; Forrest, G.; Itoh, Y.; Marsh, D. J.; McLaren, D. G.; Shen, Z.; Sonatore, L.; Carballo-Jane, E.; Craw, S.; Guan, X.; Karanam, B.; Sakaki, J.; Szeto, D.; Tong, X.; Xiao, J.; Yoshimoto, R.; Yu, H.; Roddy, T. P.; Balkovec, J.; Pinto, S. Pharmacological inhibition of diacylglycerol acyltransferase 1 reduces body weight and modulates gut peptide release: potential insight into mechanism of action. *Obesity* **2013**, *21*, 1406–1415.

(29) Inhibition of ACAT has been shown to cause adverse changes in preclinical species, see: Floettmann, J. E.; Buckett, L. K.; Turnbull, A. V.; Smith, T.; Hallberg, C.; Birch, A.; Lees, D.; Jones, H. B. ACAT-selective and nonselective DGAT1 inhibition: adrenocortical effects. A cross-species comparison. *Toxicol. Pathol.* **2013**, *41*, 941–950.

(30) For protocols measuring aqueous solubility and free fractions in plasma, see ref 24.

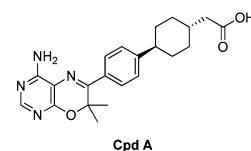
(31) For a description of mouse LTT, see ref 28.

(32) Radiolabeled MK-499 has been used in a hERG (potassium ion channel Kv11.1) binding assay to provide an initial screen of a compound's potential to interact with hERG. Blocking hERG can result in QTc prolongation, a serious adverse effect. Raab, C. E.; Butcher, J. W.; Connolly, T. M.; Karczewski, J.; Yu, N. X.; Staskiewicz, S. J.; Liverton, N.; Dean, D. C.; Melillo, D. G. Synthesis of the first sulfur-35-labeled hERG radioligand. *Bioorg. Med. Chem. Lett.* **2006**, *16*, 1692–1695.

(33) For a description of rat LTT, see Supporting Information.

(34) The plasma concentrations reported here were the concentrations of **5A** and **5B** combined at the 4 h time point postoral dosing in contrast to mouse LTT where the plasma concentrations were measured at the 20 h time point postoral dosing.

(35) The positive control, Cpd A, was originally disclosed by scientists at Japan Tobacco and Tularik: Fox, B. M.; Furukawa, N. H.; Hao, X.; Lio, K.; Inaba, T.; Jackson, S. M.; Kayser, F.; Labelle, M.; Kexue, M.; Matsui, T.; McMinn, D. L.; Ogawa, N.; Rubenstein, S. M.; Sagawa, S.; Sugimoto, K.; Suzuki, M.; Tanaka, M.; Ye, G. Yoshida, A.; Zhang, J. A. Preparation of fused bicyclic nitrogen-containing heterocycles, useful in the treatment or prevention of metabolic and cell proliferative diseases. WO 2004/ 047755A2. CAN 14138623.



(36) For a description of the food intake and body weight study, see ref 28.

(37) Mercangöz, A.; Korkmaz, F. Mutagenicity of 1-ethyl-2,4,5-triphenyl-1H-imidazole and six derivatives in *Salmonella typhimurium*. *Gazi Univ. J. Sci.* **2012**, *25*, 1–8.

(38) For an excellent discussion on in silico prediction of mutagenicity, see: Hillebrecht, A.; Muster, W.; Brigo, A.; Kansy, M.; Weiser, T.; Singer, T. Comparative evaluation of in silico systems for Ames test mutagenicity prediction: Scope and limitations. *Chem. Res. Toxicol.* **2011**, *24*, 843–854.

(39) Guidance for Industry: safety testing of drug metabolites. Center for Drug Evaluation and Research, U.S. FDA, February, 2008. <http://www.fda.gov/downloads/Drugs/GuidanceComplianceRegulatoryInformation/Guidances/ucm079266.pdf> (downloaded January 2014).